Syst. Biol. 67(5):743–755, 2018

DOI:10.1093/sysbio/syy019
Advance Access publication March 9, 2018

The Biogeography of Deep Time Phylogenetic Reticulation

FRANK T. BURBRINK* AND MARCELO GEHARA

Department of Herpetology, The American Museum of Natural History, 79th Street at Central Park West, New York, NY 10024, USA
**Correspondence to be sent to: Department of Herpetology, The American Museum of Natural History, 79th Street at Central Park West, New York, NY 10024, USA; E-mail: fburbrink@amnh.org.*

Received 18 September 2017; reviews returned 28 February 2018; accepted 05 March 2018
Associate Editor: Cecile Ane

Abstract.—Most phylogenies are typically represented as purely bifurcating. However, as genomic data have become more common in phylogenetic studies, it is not unusual to find reticulation among terminal lineages or among internal nodes (deep time reticulation; DTR). In these situations, gene flow must have happened in the same or adjacent geographic areas for these DTRs to have occurred and therefore biogeographic reconstruction should provide similar area estimates for parental nodes, provided extinction or dispersal has not eroded these patterns. We examine the phylogeny of the widely distributed New World kingsnakes (*Lampropeltis*), determine if DTR is present in this group, and estimate the ancestral area for reticulation. Importantly, we develop a new method that uses coalescent simulations in a machine learning framework to show conclusively that this phylogeny is best represented as reticulating at deeper time. Using joint probabilities of ancestral area reconstructions on the bifurcating parental lineages from the reticulating node, we show that this reticulation likely occurred in northwestern Mexico/southwestern US, and subsequently, led to the diversification of the Mexican kingsnakes. This region has been previously identified as an area important for understanding speciation and secondary contact with gene flow in snakes and other squamates. This research shows that phylogenetic reticulation is common, even in well-studied groups, and that the geographic scope of ancient hybridization is recoverable. [Hybridization; kingsnakes; Mexico; neural networks.]

The tree of life is typically represented as a purely bifurcating graph, and it naturally follows that downstream approaches to understand processes associated with the diversification of life also use these representations (Haeckel 1866; Felsenstein 2004; Pyron and Burbrink 2013; Paradis 2014). Bifurcation implicitly assumes that diversification occurs without reticulation; speciation produces two taxa that are then vertically independent of all other taxa (Coyne and Orr 2004; Mallet 2007). However, there are numerous examples of genetic introgression between two independently evolving taxa within all domains of life (Rheindt and Edwards 2011; Feder et al. 2012; Nosil 2012; Twyford and Ennos 2012; Harrison and Larson 2014; Burbrink and Guiher 2015). Alternatively, speciation via hybridization, where extant parental species have hybridized to produce morphologically and ecologically distinct taxa that are reproductively isolated from either parental taxon, is well known in prokaryotes and plants (Koonin et al. 2001; Gogarten et al. 2002; Mallet 2007; Hegarty and Hiscock 2008; Soltis and Soltis 2009; Soltis et al. 2010; Abbott et al. 2013; Schumer et al. 2014; Mallet et al. 2016) but also important examples have demonstrated this process in birds, lizards, snakes, salamanders, frogs, fishes, and insects (Hillis et al. 1987; Arnold 1997; Mallet 2005; Bogart et al. 2007; Fujita and Moritz 2009; Abbott et al. 2012, 2013; Grismer et al. 2014; Trier et al. 2014). In addition, it is common to find some gene flow between ecologically distinct sister species, suggesting that perhaps many taxa may not be free from horizontal phylogenetic connections (HPCs) after speciation (Rundle and Nosil 2005; Nosil 2008; Burbrink et al. 2011; Martin et al. 2013). Taken from the point of view that instances of hybridization or gene flow may have occurred anywhere along the tree of life, representing evolutionary history as bifurcating with purely vertical inheritance may be in error.

Several recent studies using genomic data have shown instances of deep time reticulation (DTR), where gene flow or hybridization occurred prior to clade diversification, particularly within some well-known groups: grapes (Wan et al. 2013), mosquitos (Wen et al. 2016a), clownfishes (Litsios and Salamin 2014), swordtails (Cui et al. 2013), cats (Figueiró et al. 2017), bears (Kumar et al. 2017), pigs (Frantz et al. 2013), and equids (Jónsson et al. 2014). The presence of DTR in a phylogeny, while on the surface is uninformative about the specific process of HPC, indicates that internal node diversity and subsequent clade diversification have arisen after horizontal transfer of some portion of the genome across ancestral lineages. If this is common, then DTR may be a more important process for generating biodiversity than once considered. We further underscore that all of the recent advances in comparative biology (Nee 2001; Morlon et al. 2010; Stadler 2011; Rabosky 2014) cannot therefore handle this important process methodologically or computationally. Indeed, failing to account for reticulation when estimating ecological-evolutionary processes (Harmon et al. 2008; Revell 2012; Paradis 2014; Pigot and Etienne 2015) may produce biased results by necessarily considering the data and processes as evolving on a bifurcating tree.

Unfortunately, detecting DTR is difficult while accounting for incomplete lineage sorting (ILS), where genealogies fail to coalesce within a population due to large effective population sizes (N_e) relative to divergence time (Maddison and Knowles 2006; Huson et al. 2010; Yu et al. 2011, 2014; Leaché et al. 2014;

Solís-Lemus and Ané 2016; Wen et al. 2016b). For example, a species-tree approach requires estimating ILS while simultaneously determining how much of the non-recombining genomic dataset is the result of migration (Yu et al. 2014; Solís-Lemus and Ané 2016). This contrast between migration and ILS has been addressed mainly in phylogeographic or population genetic contexts at shallow time scales (Hey 2010; Leaché et al. 2014; Burbrink and Guiher 2015), yet methods that account for DTR at more ancient phylogenetic scales are less common, likely due to the lack of methodology and required computational resources.

While detecting the signal of DTR vs. ILS could be accomplished using typical isolation-migration models using maximum likelihood, pseudolikelihood, Markov chain Monte Carlo (MCMC), or simulation approaches, parameters including population sizes, migration rates, and splitting times over a tree of many species for large genomic datasets becomes computationally difficult, particularly for unsampled ancestral populations (Hey and Nielsen 2004; Hey 2010). Alternatively, network theory, which deals with the mathematics of implicit and explicit networks, has advanced the study of estimating reticulating phylogenies (Yu et al. 2014; Francis and Steel 2015; Solís-Lemus and Ané 2016; Zhu and Degnan 2017). Implicit networks highlight statistical differences among gene trees, yet these networks may not have clear biological meaning. With respect to DTR and empirical research on complex evolutionary history and processes, only explicit networks are relevant, where reticulation represents real biological phenomena and nodes represent ancestral species. In the context of explicit networks, it was shown that the phylogenetic placement of reticulating branches and the percent contribution of genes along those branches can be determined using concordance factors (CFs), where a particular quartet is proportional to the genes that display that quartet in the true tree (Baum 2007; Solís-Lemus and Ané 2016). The expected values for CFs using coalescent models with and without reticulation are known; pure bifurcation reveals high CFs found among genes for the species tree whereas introgression mostly produces intermediate CFs deviating from expectation (Yu et al. 2011; Solís-Lemus and Ané 2016).

Because the existence of DTRs in nature have rarely been tested, it is unclear how much horizontal transfer needs to occur across taxa to be able to detect DTR. The contributions of genetic diversity to the reticulated lineage may be evenly shared between two parental taxa, as in the case where hybrid speciation has occurred (Mallet 2007; Schumer et al. 2014; Gompert et al. 2017). Hybrid speciation is considered rare (Schumer et al. 2014) and may be difficult to precisely detect for DTRs. Alternatively and more likely, contributions of genes between parental taxa may be uneven, as in the case where one parental lineage contributes more genes (the leading edge) than the other parental taxon (Baack and Rieseberg 2007; Mallet 2007; Solís-Lemus and Ané 2016).

Clearly for ancient reticulations to have occurred, ancestral species must have overlapped spatially and temporally. Indeed, to our knowledge most phylogeographic studies showing gene flow among taxa occur within geographically adjacent regions (Oliveira et al. 2015; McKelvy and Burbrink 2017; Morales and Carstens 2018). This shows that while the duration and intensity of gene flow may be unknown, it is still likely that when ranges of taxa overlap, some gene flow among species is possible. It then follows that DTR must have occurred in the same area or regionally proximate regions. For example, genomic analysis of cats show that DTR is common and likely happened in areas within Asia and South America (Li et al. 2016).

An empirical system composed of diverse and widespread taxa having a history of some gene flow is an optimal setting to explore the link between DTR and biogeography. Ideally, such a system would enable us to derive and estimate credible parameters from models that associate geography with diversification process. Snakes in the genus *Lampropeltis*, commonly referred to as kingsnakes and milksnakes, occur in the New World from Canada to Ecuador and are composed of 24 species (Ruane et al. 2014; Chen et al. 2017). Species are found throughout temperate forests, grasslands, deserts, lowland tropical rainforests, and cloud forests (Savage 2002; Ernst and Ernst 2003; Pyron and Burbrink 2009; McCranie 2011; Heimes 2016). Studies have suggested they originated in temperate North America and dispersed to the tropics during the Miocene and Pliocene (Pyron and Burbrink 2009; Chen et al. 2017). Additionally, gene flow does occur between contemporary taxa, and yet while their phylogenetic history has been examined in the context of purely bifurcating phylogenies, it is currently unknown if DTR has occurred at geographically similar regions (Burbrink et al. 2011; Myers et al. 2013; McKelvy and Burbrink 2017). Therefore, to provide a clearer understanding of when, where, and how diversification occurred in the kingsnakes throughout the New World, it is necessary to account for both bifurcation and DTR and how these processes have generated diversity in this group.

Herein, using new coalescent techniques that account for both ILS and gene flow, we test if the phylogeny of *Lampropeltis* is better represented as a purely bifurcating or reticulating tree. Where reticulation has occurred, we quantify the percentage of genes contributed from either parental lineage and determine if they are biased towards a leading edge. Finally, we ask given DTR, did this occur in the same ancestral area and at what time? We apply the new SNaQ approach to examine phylogenetic reticulation given ILS; this pseudolikelihood method leverages CFs over quartets of taxa to determine the phylogenetic location and probabilities of reticulation (Solís-Lemus and Ané 2016). We have also developed custom scripts using neural networks to apply simulations that incorporate a range of population genetic parameters allowing rapid assessment of the fit of reticulation scenarios estimated using SNaQ. Finally, we estimate ancestral area probabilities for these reticulating nodes by taking joint parental lineage probabilities using the package BioGeoBEARS (Matzke 2013; Fig. 1).

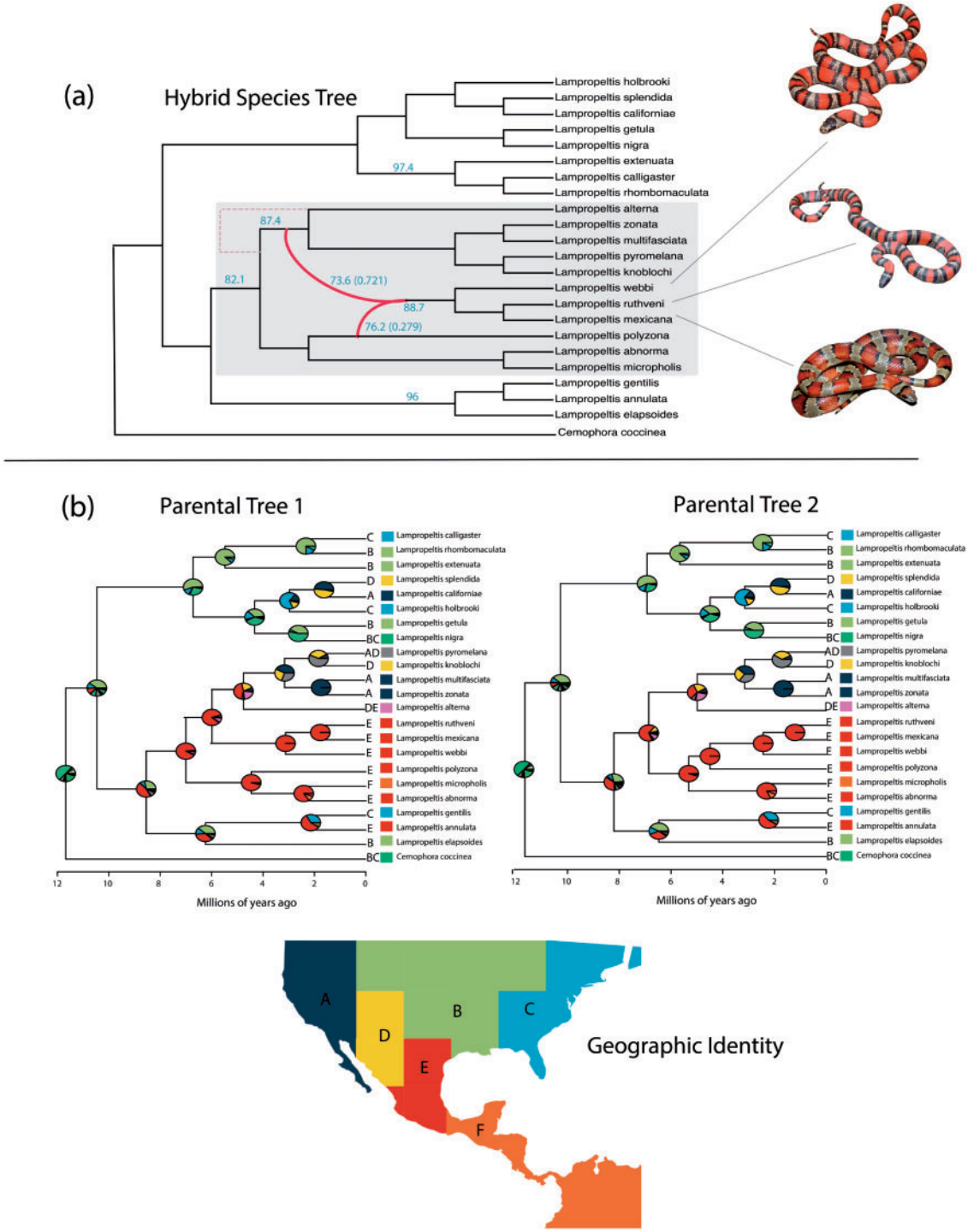

FIGURE 1. a) Phylogenetic network of *Lampropeltis*. The gray portion of the tree was used for neural network simulations (see Fig. 2 and methods for details). Tree support is shown in blue and where reticulation occurs with red branches, we show percent of the genome introgressed between major and minor sister edges. Tree support at 100% is not shown. b) Biogeographic reconstruction using the two alternative bifurcating topologies, depicted here as the major and minor sister edge topologies. Geographic areas are consistent with a = Mediterranean Californian and Pacific Northwestern, b = the Great Plains, c = Forests eastern Nearctic forests, d = Sonoran Deserts, e = Chihuahuan Desert, and f = Neotropical wet forests. Photographs of members of the hybrid clade were kindly provided by R. Hansen. From top to bottom they are: *Lampropeltis webbi*, *Lampropeltis ruthveni*, and *Lampropeltis mexicana*.

This research provides an important example of temporally and spatially proximate DTR in a widespread group of vertebrates and introduces a simulation-based approach to test for reticulation and genomic contributions from parental lineages.

Materials and Methods

Data

Anchored hybrid enrichment data were generated and aligned in Chen et al. (2017) following the procedures of Lemmon et al. (2012). We generated hundreds of long loci for 23 species of *Lampropeltis* and the outgroup *Cemophora coccinea* (Chen et al. 2017; Supplementary data available on Dryad at https://datadryad.org//resource/doi:10.5061/dryad.4qs50.

SNaQ

To estimate a phylogenetic network for *Lampropeltis*, we used SNaQ (Solís-Lemus and Ané 2016), which calculates the maximum pseudolikelihood of a network from four-taxon CFs and is implemented in the PhyloNetworks Julia package (https://github.com/crsl4/PhyloNetworks.jl). The method takes two inputs, a starting bifurcating tree and a concordance factor table. For the starting tree, we used a species tree estimated in ASTRAL II (Mirarab and Warnow 2015; Chen et al. 2017). To generate the CFs, we used BUCKy (Ané et al. 2007) through the TIRC pipeline (Stenz et al. 2015; https://github.com/nstenz/TICR). The pipeline was initiated by running MrBayes for every gene. Given that there are only a few informative sites per gene (see Results) and could only implement a single model for all genes in the TICR pipeline, we used a K2P model with a dirichlet state frequency prior. For each gene, we ran three replicates with a MCMC of 200,000 generations with three chains, a temperature of 0.40 and a swapping frequency of 10. We sampled parameters every 100 generations and discarded 25% as burn-in. We combined all three replicates and checked effective sample sizes (ESS) with the coda R-package (Plummer et al. 2006), which calculated a minimum ESS across all parameters and all runs. We then used the MrBayes output trees as inputs for BUCKy, under default parameters, to generate a four-taxon concordance factor table.

A major challenge in network estimation is to identify the optimal number of hybrid nodes supported by the data. Therefore, we ran SNaQ using a range of possible hybrid nodes from 0 to 10. For each number of hybrid nodes, we ran 10 SNaQ searches and retained the highest pseudolikelihood value. We then took all 11 pseudolikelihoods across all hybrid nodes and applied slope heuristics using the R package capushe (Baudry et al. 2012) to identify the largest change among pseudolikelihoods, which yields optimal model improvement given the increase of parameters. We also visually inspected the reticulations to evaluate if the increase in hybrid nodes represents the expected additional reticulation but with the same connections present among fewer hybrid nodes. After defining the number of reticulations, we assessed support for these using 150 bootstrap replicates which were summarized using PhyloNetworks.

Neural Network

To further explore if the *Lampropeltis* genomic data better fit a bifurcating or reticulating phylogeny, we used coalescent simulations in a machine learning (ML) classification framework. Machine learning approaches are a powerful and quick alternative to likelihood-based methods for examining complex questions that have numerous variables in population genomics (Libbrecht and Noble 2015; Sheehan et al. 2016). The power of the artificial neural networks is apparent in population genetics where numerous parameters from a non-linear system can be used to generate either simple or complex models regardless of the statistical distribution of those variables or the relationship among them (Lek et al. 1996; Zhang 2010). As in typical multi-layer feed-forward back-propagation neural network studies, the structure of the network begins with an array of our genetic input variables (input neurons), connected by weighted synapses to hidden neurons, and then finally to an output neuron. All nodes are connected to all other nodes in the previous layer, each node is given an activation value, which is the weighted sum of all inputs subtracted from a bias (threshold), and finally the connected hidden neurons activate an output node that is compared to a known (dependent) value. Herein, the output is either a bifurcating or reticulating tree. Importantly, the accuracy of the neural network is measured by comparing the output predicted by the neural network to known values from either real data or from simulations. These outcomes are used to iterate network learning by adjusting neuron and bias-weight connections to improve accuracy and produce a best-fit model (Wasserman 1989; Lek et al. 1996; Lek and Gue 1999; Basheer and Hajmeer 2000; Bryant and Shreeve 2002; Zhang 2010). This new model with associated accuracy from the previous training can then be used on new data to determine if they were produced from a bifurcating or reticulating phylogeny. We do not, however, use the neural network to infer phylogeny, which at this stage would be computationally prohibitive, but rather use the genomic data from these snakes to predict if they fit a bifurcating or reticulating phylogeny.

To simplify the simulations, we restricted the analysis to the clade representing the hybrid node and the major and minor sister groups (Figs. 1 and 2). We defined two groups representing the hybrid connections, which are the major and minor parental lineages determined from SNaQ results. Group 1 represented the major sister formed by a clade containing *L. alterna*, *L. zonata*, *L. multifasciata*, *L. pyromelana*, and *L. knoblochi* with the

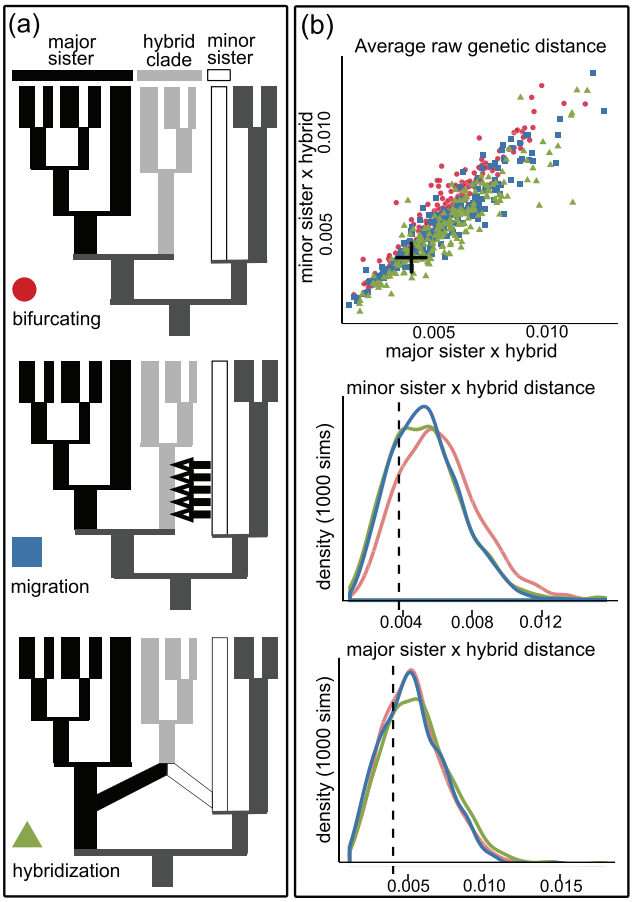

FIGURE 2. a) Schematic representation of the simulated models used to assess the probability of reticulation in Lampropeltis (see Fig. 1a). b) Plots of simulated average distances of major sister against hybrid and minor sister against hybrid with the observed value represented by the cross and the dotted line.

hybrid clade (*L. webbi*, *L. ruthveni*, and *L. mexicana*). Group 2 represented the minor sister and contained the hybrid clade plus *L. polyzona*, *L. abnorma*, and *L. micropholis*.

To generate the training data we used *ms* (Hudson 2002) to simulate 304 genes under three different models, the latter two models representing DTR (Fig. 2): (i) a bifurcating model based on the species tree estimated by ASTRAL; (ii) a hybridization model, where we took the same ASTRAL tree but added an admixture event between the area of optimal hybridization before the diversification of the hybrid clade which occurs with the minor sister, *L. polyzona,* and the ancestor of the major sister, *L. alterna*, *L. zonata*, *L. multifasciata*, *L. pyromelana*, and *L. knoblochi*; and (iii) a migration model, which was also based on the ASTRAL tree topology but included unidirectional migration from the minor sister, *L. polyzona,* to the ancestor of the hybrid clade. In reverse time, consistent with the coalescent, admixture is modeled as a split of the ancestor of the hybrid clade into two populations. The genes of the ancestor of the hybrid merge with *L. polyzona* with probability p and the second population merges with the ancestor of the major sister with probability 1-p (Fig. 2). We sampled the probability p from a uniform prior distribution (0–0.9). For modeling gene flow from ancestral migration from *L. polyzona* to the ancestral of the hybrid clade, we sampled $4N_m$ from a uniform distribution (0–1). In each replicate, all 304 loci were simulated under a single model. We sampled one N_e per population and one tMRCA per node per replicate. Only the mutation rate varied across loci. For the admixture model, we simulated all loci with one sampled admixture probability per replicate. For the gene flow model, we sampled one migration rate per replicate. Because the coalescent is a probabilistic model and the genes are unlinked, even under the two DTR models some loci will carry no signal of admixture and will still fit a history of bifurcation. The simulated models represent the history of the species, not the history of the genes. We expect to recover the true history of the species with confidence given that we are simulating 304 loci in our analysis.

For all models, divergences at the nodes were derived from the dated tree generated in BEAST (see details in the section below) and converted into generations assuming a time to sexual maturity of 2 years for all species (Burbrink et al. 2011; Ruane et al. 2014). To include variation on divergence times, we sampled the divergence of the deepest node from a uniform prior based on the lower limit of the dated species tree from Ruane et al. (2014) and the upper limit of our estimated *BEAST tree (2–11.2 Mya). Given variation at the root time, we similarly varied divergence times of more recent nodes keeping the same branch lengths proportion given by the dated tree. We assumed that N_e across species and ancestral populations was normally distributed. We allowed variation in this distribution by sampling a mean N_e from a uniform prior (min: 50,000; max: 1,000,000). We also allowed the standard deviation (SD) to be from 10× smaller up to the same value as the mean. To generate SD, we took the sampled N_e and multiplied this value by a number drawn from a uniform prior (min: 0.1; max: 1). We used the same approach to allow variation in the mutation rates across genes. We sampled a mean mutation rate from a uniform distribution (min: 1×10^{-10}; max: 1×10^{-9}), multiplied that value by a number range (0.1–1.0) to generate the SD, and then drew mutation rates for the 304 genes from a normal distribution generated from the two previously sampled parameters. We also allowed the length of genes to vary by sampling from the empirical distribution of number of base pairs across our 304 genes (mean = 1489; SD = 285). All normal distributions were truncated at zero.

In each simulation cycle under each model, we calculated the pairwise proportion of base pair differences between all combinations of terminal taxa totaling 55 genetic distances across all 304 genes. We expect to have a lower genetic distance between species from the hybrid clade and species from the major and minor sister clades in the DTR models, and a larger distance in the bifurcating model. We repeated the simulations 10,000 times for each model to generate a reference data set of

30,000 samples for training and testing a neural network classification algorithm. Before training the algorithm, we calculated the 55 distances in our observed data and ensured a good model fit for the three models using the *gfit* function from the abc R-package (Csilléry et al. 2012). For every model, we also plotted all 55 simulated distances against the observed values to visually inspect if the simulated values encompassed the observed. We implemented the ML approach using the *nnet* method in the training functions of the caret R package (Kuhn 2008). We took 75% of the simulated data for training and 25% for testing the ML classification using the function *train*. Before training we scaled and centered the data and used a bootstrapping resampling method with 10 iterations to tune parameters. We selected the optimal tuning parameters by evaluating the accuracy of model classifications across replications. We then used the remaining 25% of simulations as test data to calculate the final accuracy of the classification algorithm; this trained algorithm was used to determine if our empirical data best fit a bifurcation, hybridization or gene flow model.

Effective population size may influence the genetic distance between species. For instance, if two recently diverged species have a large N_e, ancestral polymorphism will likely be retained in several genes decreasing the overall genetic distance between them. Thus, a large population size in the minor sister could generate a signal similar to reticulation, where the genetic distance is shorter than expected by bifurcation. To account for that bias, we explored the effect of forcing the N_e of *L. polyzona* to be $10\times, 100\times$, and $1000\times$ larger than the average N_e across populations on the bifurcating model. We performed 1000 simulations for each N_e and tested these models against the hybridization model.

Although neural networks are suited for either low or high dimensional data with either simple or complex solutions, we also ran the same training approach as above but with two reduced feature tables: one containing only the pairwise distances that have a correlation lower than 0.95 and another data set containing only the average distance between major and minor sister groups and the hybrid clade (Fig. 2). All simulation code used in this analysis was developed in R and is available as part of the flexible PipeMaster package in github (www.github.com/gehara/PipeMaster).

Neural Network Regression

For each simulated model, we also performed a neural network regression to estimate parameters for our empirical data. For all three models, we estimated: (i) the age at the root of the simulated clade (Fig. 2); (ii) the average effective population size across all species; (iii) the SD of the population sizes; (iv) the average mutation rate, and (v) the SD of the mutation rate. For the hybridization model, we also estimated the admixture proportion; and for the gene flow model we estimated the migration rate. For each model, we trained the neural network using all 55 features and 75% of the simulations. We performed the same training and testing setup as above but we used the coefficient of determination (r^2) to select the best tuning parameters across replicates. We then tested the performance of the neural network with the remaining 25% of the data and estimated the parameters of the models.

Divergence Dating

To produce chronograms suitable for ancestral area estimation and neural network simulations, we first split the hybrid-species trees into the two parental bifurcating trees. We then estimated divergence dates on these fixed phylogenies using the concatenated anchored hybrid enrichment data under a GTR+Γ+I model of substitution in *BEAST with a relaxed lognormal clock. We calibrated the node that splits *Cemophora* from *Lampropeltis* based on the oldest fossil, *Lampropeltis similis* from the Barstovian of the Miocene, yielding a mean date 13.75 Ma (95% HPD 8.4–24.4; for using this fossil in a phylogenetic context see Holman 1964; Myers et al. 2013; Ruane et al. 2014). For each of the two topologies, we ran these analyses for 50×10^6 generations, thinned by every 5000 trees and excluding the first 5×10^6 as burn in, generating ESS values >2000 (Supplementary Data available on Dryad).

Ancestral Area

We examined ancestral area to determine if the reticulating edges occurred in the same regions. To obtain unbiased estimates of the range for each taxon, species were first georeferenced from sources VertNet (vertnet.org) and Ruane et al. 2014. We examined 2719 georeferenced localities for all species of *Lampropeltis* and *Cemophora*, removing replicates and species localities in error from their known range (Supplementary data for georeferenced specimens available on Dryad). From these points, we used the InfoMap Bioregions (Edler et al. 2017), which takes locality information for species distributions, to generate bioregion maps using network theory. We generated six objective biogeographic regions for testing ancestral area using a standard cluster cost of 1.7 at a 16′ max cell size resolution over 10 trials. We standardized the identity of each taxon to bioregions by constraining the count of occurrences to be greater than 5% of the total distribution of occurrences so that outliers were not present in all regions.

We then used BioGeoBEARS (Matzke 2013) to estimate probabilities for all ancestral areas using (i) the extant area(s) coded for each taxon and (ii) each bifurcating phylogeny. For each of the two parental bifurcating phylogenies, one with the major sister edge and the other with the minor sister edge (Fig. 1), we determined the most likely model for estimating ancestral area among the following candidates: DEC, DEC+J, DIVALIKE, DIVALIKE+J, BAYAREALIKE, and BAYAREALIKE+J.

From the model with lowest AIC, we then estimated ancestral area probabilities across each phylogeny.

Finally, for nodes generated by DTR, we calculated the joint probability for each ancestral area on the corresponding bifurcating tree giving rise to these internally connected edges and ranked these likelihoods for each region. The expectation is that nodes for each reticulating edge should be spatially overlapping if substantial gene flow occurred between these lineages (Supplementary Data for BioGeoBEARS code and all input data available on Dryad).

Schematic representation of work flow from SNaQ, neural network simulations, and ancestral area estimation available as a Supplementary Fig. S1 available on Dryad.

Results

Data

We generated 304 loci for 23 taxa with an average alignment size of 1489 bp (range 509–2224, SD = 289), and an average number of parsimony informative sites of 13.07 (SD = 7.8). Most loci produced some phylogenetic signal; we found that Robinson–Foulds (RF) distances for each locus ranged from 18 to 40 (mean = 32) from the species tree relative to a maximum RF of 40. As in Chen et al. (2017), we found that 97% of loci matched to known genes from the *Python bivittatus* genome (Castoe et al. 2011).

Support for DTR

The slope heuristics on outputs from SNaQ indicated two values for the best number of hybrid connections, 1 and 6 (Supplementary Fig. S2 and Table S1 available on Dryad). Although it cannot distinguish between these two values, it indicates that a bifurcating topology has a poor fit to the data, where pseudolikelihoods for 0 hybrid nodes differed at a minimum of 7989 pseudolikelihood units compared to any topology with reticulation. Additionally, the location of one reticulation is similar in trees with 1 or 6 hybrid connections, though the latter adds five additional connections (Supplementary Fig. S3 available on Dryad). Therefore, we assumed that the topology with a single hybrid should provide a good representation of the relationships within *Lampropeltis* without over parameterizing the phylogeny.

The resulting network with one reticulation showed the hybrid clade containing the three species: *L. webbi*, *L. ruthveni*, and *L. mexicana*. The major sister clade was composed of *L. alterna*, *L. zonata*, *L. multifasciata*, *L. pyromelana* and *L. knoblochi*, and on average contributes with 72% of the genes. The minor sister lineage, represented by *L. polyzona*, contributes 28% of their genes to the hybrid clade. The bootstrap support across 150 replicates for this reticulation is 88.7 for the major sister clade (Fig. 1), which is slightly different across replicates given the occasional exclusion of *L. alterna* from the major sister clade (10% of the time).

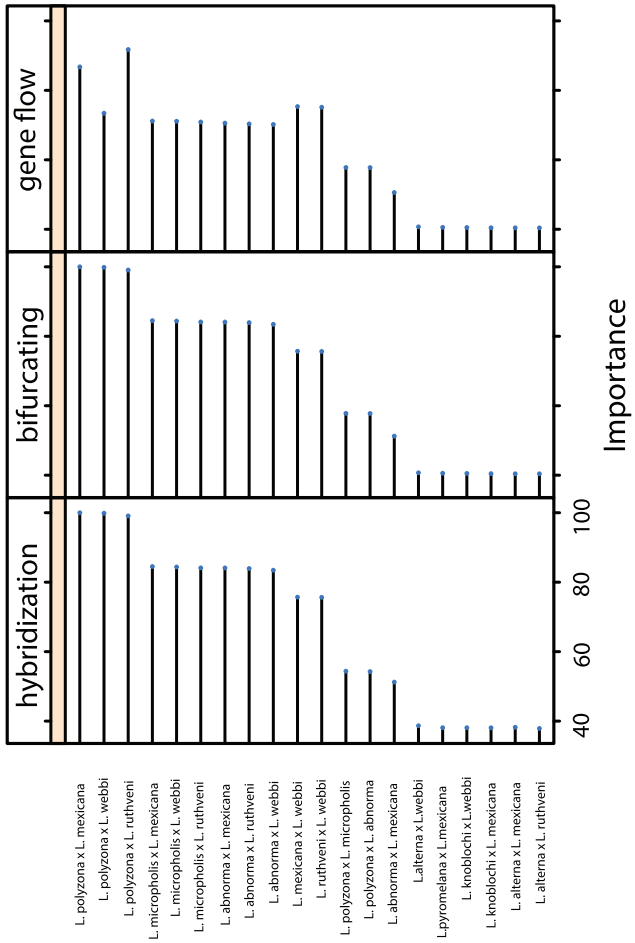

FIGURE 3. Scaled variable importance for genetic distances among *Lampropeltis* for the three neural network models. Highest variable importance always involves a member of the reticulating clade (*L. webbi*, *L. ruthveni*, and *L. mexicana*) and either major or minor edge sister group or taxon.

Neural Network

Our neural network can classify the three models with 0.82 accuracy when using the 55 data features (pairwise distances). It also ranked the genetic pairwise distances between species forming the hybrid clade with one of the sister groups as the most important feature for data classification (Fig. 3). Our empirical data were classified as a network diversification model in all three cases with a complete set of genetic distances (55) and the two sets of reduced distances (10 and 2; Table 1), which confirmed the results from the SNaQ analysis. The migration model has the highest probability when incorporating all 55 distances. When the parameters were reduced, the hybridization and gene-flow models had similar probabilities. Both the migration and hybridization models generated a lower distance between *L. polyzona* (minor edge) and the hybrid clade in comparison to the

TABLE 1. Model probabilities, accuracy, and kappa calculated with the trained neural network

	Model probability			Accuracy	Kappa
	Bifurcating	Hybridization	Gene flow		
55 variables	0.00	0.00	1.00	0.82	0.73
10 variables	0.00	0.58	0.42	0.71	0.56
2 variables	0.01	0.50	0.49	0.59	0.39

The 55 variables represent the pairwise distance across 11 tips. The 10 variables represent the pairwise distance with correlation lower than 0.95. The two variables are the average distance between the major sister clade and the hybrid clade and the average distance between the minor sister clade and the hybrid clade.

TABLE 2. Neural network regression and r^2 for model parameters, root height, effective population size (N_e), mutation rate (μ), and migration/admixture rate, under each simulated model[a]

	Bifurcation		
	Estimate	RMSE	r^2
Root height	7,139,156	1,440,038	0.71
N_e (mean)	763,732	235,033	0.82
N_e (SD)	364,296	280,588	0.59
μ(mean)	2.40E−10	8.84E−11	6.28E−07
μ(SD)	1.36E−10	9.02E−11	7.01E−04
	Gene flow		
Root height	5,489,993	1,398,295	0.72
N_e (mean)	782,709	223,399	0.83
N_e (SD)	371,840	284,915	0.56
μ(mean)	2.55E−10	8.67E−11	1.41E−03
μ(SD)	1.29E−10	8.47E−11	1.42E−03
Minor mig. Rate ($4N_m$)	0.95	0.18	0.60
	Hybridization		
Root height	7,643,680	1,399,671	0.72
N_e (mean)	445,615	220,309	0.84
N_e (SD)	209,149	289,109	0.55
μ(mean)	2.59E−10	8.91E−11	2.08E−04
μ(SD)	1.42E−10	8.31E−11	8.25E−05
Minor admix. prop.	0.32	0.09	0.87

[a]We define the units for the following variables: root height = years, N_e = number of individuals, μ = substitution/site/year, and migration rate is in migrants per generation.

bifurcating model (Fig. 2). This plot also showed that both gene flow and hybridization models overlap for the two reduced variables, which explains the low accuracy and similar probabilities when the inputs were abridged.

We also note that although the N_e affects the distance between *L. polyzona* and the other species, slightly decreasing the accuracy of model classification, the change was not substantial enough to confound the hybridization model and the bifurcating model. Resulting accuracy for all the pairwise classifications (larger N_e vs. hybridization) is always higher than 85%.

The neural network regression yielded a high r^2 for the root height, mean N_e, and admixture proportions. The estimated root height of the simulated clade varied from 5.5 to 7.6 Ma and the mean N_e ranged from 445,615 to 782,709 depending on the model (Table 2). The estimated admixture proportion of the minor edge was remarkably concordant with the SNaQ analysis and suggest a contribution of 32%.

Divergence Dating and Biogeographic Reconstruction

Genomic data fitted to both parental bifurcating phylogenies generates ESS values >2000. Phylogenetic structure and dates were largely similar to Ruane et al. (2014) and the fossil record of North American snakes in general (Holman 2000) showing that *Lampropeltis* originated in the mid-Miocene and most species-level divergences occurred within the Pliocene or Pleistocene. BEAST estimated the timing for the MRCA of both parental nodes and the hybrid clade occurring between 4.52 and 5.78 Ma (combined bifurcating trees 95% HPD 2.58–8.6 Ma) and the origin of the MRCA of the hybrid clade alone between 2.4 and 2.73 Ma (combined bifurcating trees 95% HPD 1.23–4.5 Ma). Both parental bifurcating trees were then used to reconstruct ancestral areas (Fig. 1).

The six bioregions predicted for *Lampropeltis* by InfoMap were similar to the broad ecogeographic regions of the New World, which include the eastern Nearctic forests, the Great Plains, Chihuahuan and Sonoran Deserts, Mediterranean Californian and Pacific Northwestern forests, and Neotropical wet forests (Fig. 1; Bailey 1995; https://www.epa.gov/eco-research/ecoregions-north-america). These distributions were then used to code the ranges of extant taxa. Ancestral areas were estimated with the DEC+J model (ΔAIC >2.7) for both trees using BioGeoBEARS. This model accounts for dispersal, extinction, and the jump parameter.

For the ancestral origin of the two lineages contributing to the reticulation, we estimated the following probabilities: (i) the major sister, *L. webbi*, *L. ruthveni*, and *L. mexicana* sister to *L. alterna*, *L. multifasciata*, *L. pyromelana*, and *L. knoblochi*, was predicted to include northwestern Mexico/southwestern US with a probability 0.95; (ii) the minor sister, *L. polyzona* sister to *L. webbi*, *L. ruthveni*, and *L. Mexicana,* was predicted to be in northwetern Mexico/ southwestern US with a probability of 1.0. This indicated that the joint probability of the hybridization event occurred in Northern Mexico at 0.95 (Fig. 1; Supplementary Table S2 available on Dryad).

DISCUSSION

We show that the phylogeny of the kingsnakes, *Lampropeltis*, cannot be represented as purely bifurcating (Figs. 1 and 2; Table 1; Supplementary Figs. S2 and S3 available on Dryad). This is supported by SNaQ and by our neural network model selection approach (Fig. 2). Similarly, relationships within Mexican kingsnakes have been unstable and difficult to estimate with confidence using traditional bifurcating phylogenetic methods (Bryson et al. 2007; Ruane et al. 2014; Chen et al. 2017). Herein, we show a clear example where the phylogeny of kingsnakes is best represented with at least one DTR. This DTR likely occurred in northwestern Mexico and southwestern US which is currently a suture zone where other snake species show signs of hybridization

(Fig. 1; Myers et al. 2017). Our analysis indicates that this DTR happened near the beginning of the Pleistocene, suggesting that this suture zone may have existed in northwestern Mexico over many glacial cycles and has likely influenced the diversification of these snakes there.

Using two complimentary approaches we demonstrate that reticulation occurs between *L. polyzona* and a clade containing *L. pyromelana, L. knoblochi, L. zonata, L. multifasciata* (and possibly *L. alterna)* to produce the clade that diversifies into *L. ruthveni, L. mexicana*, and *L. webbi*. The first approach using SNaQ assesses the pseudolikelihood and location of the reticulation on the phylogeny, given expectations of ILS with hybridization, and uses bootstrapping to support each node of the parental groupings and the reticulating nodes. The support for this reticulating node was moderate relative to typical bootstraps for bifurcating phylogenies (Felsenstein 1985; Felsenstein and Kishino 1993), therefore, we developed a second modeling approach using population genetic simulations to train a neural network to classify the data under pure bifurcation or reticulation. We show strong support for the initial phylogeny inferred from SNaQ and suggest that this dual procedure for rejecting a bifurcation-only scenario is valid and could easily be adopted by other studies.

The neural network regression r^2 indicates that some parameters of the model can be inferred with confidence, such as the age of the root, the average population size, and the admixture proportion. This indicates that the genomic data used here contains information to estimate the parameters of the simulated coalescent models. However, the average mutation rate cannot be estimated. Since divergence times and population sizes are scaled by mutation rate, estimates for these parameters depend on the validity of the assumed mutation rates. Conclusions would change if future studies show unexpected average mutation rates of orders of magnitude higher or lower than those used here, though we note that our conclusions are broadly similar with those using estimates on bifurcating topologies using BEAST.

While we strongly detect only a single reticulating event during the late Neogene/Early Pleistocene among taxa distributed in southwestern US and northwestern Mexico, it is possible that other events with a lower fraction of genomic introgression may have occurred (see other trees in Supplemental Fig. S3 available on Dryad). Within *Lampropeltis* though, we find support for a migration model showing that genomic contributions between ancestral taxa are not balanced; there is always a leading edge contributing most of the genome. The lack of balance poses an essential yet unresolved problem for phylogenetic representation: how much of the ancestral genome must be involved in reticulation for that area of the tree to not be considered bifurcating? Clearly, answers must consider what is being represented with regard to both evolutionary history (Mallet et al. 2016) and important secondary efforts such as investigating the origins of traits and biogeographic reconstruction. The most accurate representation of the tree of life should depict any minor reticulation, however, practical considerations might only include those where the reticulation results in more substantial transfer of both genes and phenotype. With greater sampling of the genome and the likelihood for ancient hybridization occurring prior to terminal edges of the tree (Cui et al. 2013; Jónsson et al. 2014; Figueiró et al. 2017; Kumar et al. 2017), it is probable that smaller fractions of the genome can be detected as reticulating. For instance, here with a typical *Lampropeltis* genome size of 2.72 GBp (De Smet 1981), even 0.1% horizontal gene transfer would still result in the introgression of 270 Mbp.

Biogeography

Ancestral area reconstructions for these snakes show that reticulation occurred in northwestern Mexico and the southwestern US in the late Neogene/early Pleistocene. The origin of this reticulation agrees with the date and location of the uplift of the Sierra Madre Occidental during the Neogene and the formation of the Chihuahuan and Sonoran Deserts (Riddle and Hafner 2006; Wilson and Pitts 2010; Myers et al. 2017). While it is not clear in *Lampropeltis* how this region promoted introgression, this study is consistent with research on pairs of sister species in this area where hybridization is common and likely influenced by climate; connections between the Chihuahua and Sonoran Deserts increased during xeric times and decreased during mesic times (Morafka 1977; McGuire et al. 2007; Pyron and Burbrink 2010; Klicka et al. 2016; Myers et al. 2017). For instance, a study on crotaphytid lizards (McGuire et al. 2007) demonstrated a mtDNA introgressive conveyer system where repeated bouts of hybridization occurred at glacial maxima during the Pleistocene. Previously, it was shown that mtDNA introgression occurs between distinct species of *Lampropeltis* in the southwestern US (Ruane et al. 2014). Myers (pers. comm) indicated that secondary contact and gene flow between snake taxa at this suture zone was common throughout the Pleistocene.

We stress that biogeography could minimally serve as an independent test of phylogenetic reticulation, where biogeographic reconstructions from each parental lineage should yield the same or adjacent areas. Coding areas for ancestral area analyses should be chosen objectively given that the number of regions will likely influence the probability of detecting concordant ancestral areas among hybridizing clades. Also, given the number of ancestral areas reconstructed, it is possible that inferred adjacent areas among DTR nodes may not be statistically significant relative to a random probability of recovering the same geographic or adjacent areas over the entire tree.

Importantly, successfully recovering the same region of reticulation for parental lineages may be related to the relatively young date for the DTR. Other scenarios where

DTR might have occurred at very ancient times may prove difficult for accurately recovering the location of reticulation, particularly if both dispersal and extinction were high. Considering that event-based methods for generating ancestral area probabilities requires estimates of extinction and dispersal (Ree and Smith 2008; Matzke 2013), we expect that recovering proximate areas of overlap may be difficult for ancient DTR given that estimating extinction rates is often problematic when using only molecular phylogenies (Quental and Marshall 2010; Rabosky 2010). However, alternate models of area reconstruction over different rates of extinction and dispersal are testable for every node (Clark et al. 2008; Ree and Smith 2008; Matzke 2014). We note that estimating the joint probability of reticulating ancestral areas in the kingsnakes was trivial given this probability included only two parental trees, however difficulty estimating ancestral area is likely to increase with greater numbers of terminal taxa and reticulations and the potential for more than two contributors per node. On the other hand, it is also likely that finding ancient introgression in the genomes of geographically disparate taxa could provide evidence of shared ancestral areas, even in the absence of phylogenetic reconstruction of these areas.

This DTR in *Lampropeltis* in northwestern Mexico led to the diversification of additional species, likely broadening the niche of the entire group. This process, where introgression or hybridization facilitates adaptive radiation by providing a wider range of genetic variation and allelic combinations (Seehausen 2004) is being realized in other species like Lake Victorian cichlids (Meier et al. 2017). Within the kingsnakes, reticulation and subsequent diversification produced most *Lampropeltis* species now occupying the southern North America in Mexico near the transition with the Neotropics. These examples demonstrate that detecting the phylogenetic and biogeographic location of reticulation provides a better understanding and a platform for addressing how introgression or hybridization has contributed to the adaptive radiation of a group beyond simple bifurcation, which may not capture the entirety of processes leading to the standing diversity.

Estimating Dates of Reticulation

Event-based methods of ancestral area reconstruction require dated trees to connect the spatial and temporal dimensions for hypothesis testing (Ronquist 1997; Matzke 2013). Binding the time of reticulation given the MRCA of parental and hybrid nodes and subsequent species diversification in the hybrid node appears simple and only requires fitting data and estimating dates on the bifurcating parental trees. However, this solution is not optimal since it does not specifically date the timing of reticulation. Using simulations and neural network regression, we confirmed that the dates estimated by BEAST were consistent under the coalescent without data concatenation (Table 2). Nevertheless, we only allowed node heights to vary proportionally in our simulations, this means that the divergence times were not independent from one another. Thus, the reticulation time was still bounded by minimum and maximum dates from relatively deeper and shallower nodes, respectively.

Future studies should develop methods that account for reticulation, their location, and their effects on divergence estimates analytically. Leaché et al. (2014) demonstrated that species compression, where divergence dates are underestimated, and species dilation, where population sizes are overestimated, commonly occurs with some gene flow when analyzing dates only using multispecies coalescent methods that do not account for migration. This may have happened in the kingsnake example here, though dates of reticulation are estimated consistently with appreciable error to the late Miocene/late Pliocene. Depending on the location of calibration points and the reticulation, species compression may affect date estimates throughout the entire phylogeny.

Comparative Phylogenetics

If phylogenetic reticulation is common across the tree of life, then comparative phylogenetic methods must be updated to use these trees. Authors in this special issue on phylogenetic reticulation in Systematic Biology have made steps towards addressing the problem for Brownian motion-based ancestral trait estimation in the face of reticulation (Bastide et al. 2018, O'Meara et al. 2018). However, solving comparative phylogenetic problems using reticulating phylogenies will require methods to incorporate trait evolution using all models beyond Brownian motion (e.g., AC/DC, Ornstein–Uhlenbeck), time dependent or independent methods of diversification, trait-driven diversification, disparification, community phylogenetics, and ancestral area reconstruction (Harmon et al. 2008; Ree and Smith 2008; Cavender-Bares et al. 2009; FitzJohn et al. 2009; Revell 2012; Pyron and Burbrink 2013; Paradis 2014). We envision that new methods for incorporating reticulation will advance our understanding of how trait diversification and speciation occur via hybridization, particularly in the special case where reticulation ultimately results in adaptive radiation and subsequent increases in species diversification. In cases where reticulation has led to an adaptive radiation either by simply increasing morphological and ecological diversity (Rabosky 2017) of a clade or by reducing gene flow and elevating speciation rates (Schluter 2000; Losos 2010; Burbrink et al. 2012), there are yet no tests that account for these changing rates of speciation, extinction, or traits (Alfaro et al. 2009; FitzJohn 2010; Rabosky 2014) across trees showing reticulation. We envision that new techniques will allow us to compare reticulating and bifurcating nodes throughout a network to determine if rates of speciation, morphological change or disparification are elevated where introgression occurred in the deep past in a particular geographic area, thus supporting the theory

that hybridization may lead to enhanced diversification (Seehausen 2004).

Supplementary Material

Data available from the Dryad Digital Repository: https://datadryad.org//resource/doi:10.5061/dryad.4qs50.

Funding

This work was provided by the American Museum of Natural History and was supported in part by a US National Science Foundation [DEB 1257926 to F.T.B.].

Acknowledgments

We thank Cécile Ané for helping to organize the Spotlight Session on phylogenetic reticulation at the 2017 Society for Systematic Biologists meeting in Portland, Oregon and also thank the other participants in that symposium. We are grateful to Bob Hansen for providing edits to the proofs and photographs of Mexican kingsnakes. We are indebted to Xin Chen who provided some of the data used here from Chen et al. (2017).

References

Abbott R., Albach D., Ansell S., Arntzen J.W., Baird S.J.E., Bierne N., Boughman J., Brelsford A., Buerkle C.A., Buggs R., Butlin R.K., Dieckmann U., Eroukhmanoff F., Grill A., Cahan S.H., Hermansen J.S., Hewitt G., Hudson A.G., Jiggins C., Jones J., Keller B., Marczewski T., Mallet J., Martinez-Rodriguez P., Möst M., Mullen S., Nichols R., Nolte A.W., Parisod C., Pfennig K., Rice A.M., Ritchie M.G., Seifert B., Smadja C.M., Stelkens R., Szymura J.M., Väinölä R., Wolf J.B.W., Zinner D. 2013. Hybridization and speciation. J. Evol. Biol. 26:229–246.

Abbott R.J., Rieseberg L.H., Abbott R.J., Rieseberg L.H. 2012. Hybrid speciation. eLS. Chichester, UK: John Wiley & Sons, Ltd.

Alfaro M.E., Santini F., Brock C., Alamillo H., Dornburg A., Rabosky D.L., Carnevale G., Harmon L.J. 2009. Nine exceptional radiations plus high turnover explain species diversity in jawed vertebrates. Proc. Natl. Acad. Sci. USA 106:13410–13414.

Ané C., Larget B., Baum D.A., Smith S.D., Rokas A. 2007. Bayesian estimation of concordance among gene trees. Mol. Biol. Evol. 24: 412–426.

Arnold M.L. 1997. Natural hybridization and evolution. Oxford: Oxford University Press.

Baack E.J., Rieseberg L.H. 2007. A genomic view of introgression and hybrid speciation. Curr. Opin. Genet. Dev. 17:513–8.

Bailey R.G. 1995. Description of the ecoregions of the United States. USDA Forest Service. Available from: URL https://www.fs.fed.us/rm/ecoregions/products/map-ecoregions-united-states/.

Basheer I.A., Hajmeer M. 2000. Artificial neural networks: fundamentals, computing, design, and application. J. Microbiol. Methods. 43:3–31.

Baudry J.-P., Maugis C., Michel B. 2012. Slope heuristics: overview and implementation. Stat. Comput. 22:455–470.

Baum D.A. 2007. Concordance trees, concordance factors, and the exploration of reticulate genealogy. Taxon 56:417–426.

Bogart J.P., Bi K., Fu J., Noble D.W.A., Niedzwiecki J. 2007. Unisexual salamanders (genus *Ambystoma*) present a new reproductive mode for eukaryotes. Genome 50:119–36.

Bryant S.R., Shreeve T.G. 2002. The use of artificial neural networks in ecological analysis: estimating microhabitat temperature. Ecol. Entomol. 27:424–432.

Bryson Jr. R.W., Pastorini J., Burbrink F.T., Forstner M.R.J. 2007. A phylogeny of the *Lampropeltis mexicana* complex (Serpentes: Colubridae) based on mitochondrial DNA sequences suggests evidence for species-level polyphyly within *Lampropeltis*. Mol. Phylogenet. Evol. 43: 674–684.

Burbrink F.T., Guiher T.J. 2015. Considering gene flow when using coalescent methods to delimit lineages of North American pitvipers of the genus *Agkistrodon*. Zool. J. Linn. Soc. 173:505–526.

Burbrink F.T.T., Chen X., Myers E.A.A., Brandley M.C.C., Pyron R.A.A. 2012. Evidence for determinism in species diversification and contingency in phenotypic evolution during adaptive radiation. Proc. R. Soc. B Biol. Sci. 279:4817–4826.

Burbrink F.T., Yao H., Ingrasci M., Bryson R.W.W., Guiher T.J.J., Ruane S. 2011. Speciation at the Mogollon Rim in the Arizona Mountain Kingsnake (*Lampropeltis pyromelana*). Mol. Phylogenet. Evol. 60: 445–454.

Castoe T.A., de Koning A.J., Hall K.T., Yokoyama K.D., Gu W., Smith E.N., Feschotte C., Uetz P., Ray D.A., Dobry J., Bogden R., Mackessy S.P., Bronikowski A.M., Warren W.C., Secor S.M., Pollock D.D. 2011. Sequencing the genome of the Burmese python (*Python molurus bivittatus*) as a model for studying extreme adaptations in snakes. Genome Biol. 12:406.

Cavender-Bares J., Kozak K.H., Fine P.V.A., Kembel S.W. 2009. The merging of community ecology and phylogenetic biology. Ecol. Lett. 12:693–715.

Chen X., Lemmon A.R., Lemmon E.M., Pyron R.A., Burbrink F.T. 2017. Using phylogenomics to understand the link between biogeographic origins and regional diversification in ratsnakes. Mol. Phylogenet. Evol. 111:206–218.

Clark J.R., Ree R.H., Alfaro M.E., King M.G., Wagner W.L., Roalson E.H. 2008. A comparative study in ancestral range reconstruction methods: retracing the uncertain histories of insular lineages. Syst. Biol. 57:693–707.

Coyne J.A., Orr H.A. 2004. Speciation. Sunderland: Sinnauer Associates Inc.

Csilléry K., François O., Blum M.G.B. 2012. abc: an R package for approximate Bayesian computation (ABC). Methods Ecol. Evol. 3:475–479.

Cui R., Schumer M., Kruesi K., Walter R., Andolfatto P., Rosenthal G.G. 2013. Phylogenomics reveals extensive reticulate evolution in *Xiphophorus* fishes. Evolution. 67:2166–79.

Edler D., Guedes T., Zizka A., Rosvall M., Antonelli A. 2017. Infomap bioregions: interactive mapping of biogeographical regions from species distributions. Syst. Biol. 66:197—204.

Ernst C.H., Ernst E.M. 2003. Snakes of the United States and Canada. Washington, DC: Smithsonian Books.

Feder J.L., Egan S.P., Nosil P. 2012. The genomics of speciation-with-gene-flow. Trends Genet. 28:342–350.

Felsenstein J. 1985. Confidence limits on phylogenies: an approach using the bootstrap. Evolution 39:783–791.

Felsenstein J. 2004. Inferring phylogenies. Sunderland (MA): Sinauer Associates.

Felsenstein J., Kishino H. 1993. Is there something wrong with the bootstrap on phylogenies? A reply to Hillis and Bull. Syst. Biol. 42:193.

Figueiró H. V, Li G., Trindade F.J., Assis J., Pais F., Fernandes G., Santos S.H.D., Hughes G.M., Komissarov A., Antunes A., Trinca C.S., Rodrigues M.R., Linderoth T., Bi K., Morato R.G., Loska D., Saragüeta P., Gabaldón T., Oliveira G., Murphy W.J., Eizirik E. 2017. Genome-wide signatures of complex introgression and adaptive evolution in the big cats. Sci. Adv. v. 2017;3: e1700299.

FitzJohn R.G. 2010. Quantitative traits and diversification. Syst. Biol. 59:619–633.

FitzJohn R.G., Maddison W.P., Otto S.P. 2009. Estimating trait-dependent speciation and extinction rates from incompletely resolved phylogenies. Syst. Biol. 58:595–611.

Francis A.R., Steel M. 2015. Which phylogenetic networks are merely trees with additional arcs? Syst. Biol. 64:768–777.

Frantz L.A., Schraiber J.G., Madsen O., Megens H.-J., Bosse M., Paudel Y., Semiadi G., Meijaard E., Li N., Crooijmans R.P., Archibald A.L.,

Slatkin M., Schook L.B., Larson G., Groenen M.A. 2013. Genome sequencing reveals fine scale diversification and reticulation history during speciation in *Sus*. Genome Biol. 14:R107.
Fujita M.K., Moritz C. 2009. Origin and evolution of parthenogenetic genomes in lizards: current state and future directions. Cytogenet. Genome Res. 127:261–272.
Gogarten J.P., Doolittle W.F., Lawrence J.G. 2002. Prokaryotic evolution in light of gene transfer. Mol. Biol. Evol. 19:2226–38.
Gompert Z., Mandeville E.G., Buerkle C.A. 2017. Analysis of population genomic data from hybrid zones. Annu. Rev. Ecol. Evol. Syst. 48: 207–229.
Grismer J.L., Bauer A.M., Grismer L.L., Thirakhupt K., Aowphol A., Oaks J.R., Wood P.L., Onn C.K., Thy N., Cota M., Jackman T. 2014. Multiple origins of parthenogenesis, and a revised species phylogeny for the Southeast Asian butterfly lizards, *Leiolepis*. Biol. J. Linn. Soc. 113:1080–1093.
Haeckel E. 1866. Generelle Morphologie der organismen allgemeine grundzuge der organischen formen-wissenschaft, mechanisch begrundet durch die von Charles Darwin. Berlin: G. Reimer.
Harmon L.J., Weir J.T., Brock C.D., Glor R.E., Challenger W. 2008. GEIGER: investigating evolutionary radiations. Bioinformatics 24: 129–131.
Harrison R.G., Larson E.L. 2014. Hybridization, introgression, and the nature of species boundaries. J. Hered. 105:795–809.
Hegarty M.J., Hiscock S.J. 2008. Genomic clues to the evolutionary success of polyploid plants. Curr. Biol. 18:R435–R444.
Heimes P. 2016. Snakes of Mexico. Edition Chimaira. Frankfurt: Andreas S. Braham.
Hey J. 2010. Isolation with migration models for more than two populations. Mol. Biol. Evol. 27:905–920.
Hey J., Nielsen R. 2004. Multilocus methods for estimating population sizes, migration rates and divergence time, with applications to the divergence of *Drosophila pseudoobscura* and *D. persimilis*. Genetics 167:747–760.
Hillis D.M., Collins J.T., Bogart J.P. 1987. Distribution of diploid and tetraploid species of gray tree frogs (*Hyla chrysoscelis* and *Hyla versicolor*) in Kansas. Am. Midl. Nat. 117:214–217.
Holman J.A. 1964. Fossil snakes from the Valentine formation of Nebraska. Copeia 1964:631–637.
Holman J.A. 2000. Fossil snakes of North America: origin, evolution, distribution, paleoecology. Bloomington: Indiana University Press.
Hudson R.R. 2002. Generating samples under a Wright-Fisher neutral model of genetic variation. Bioinformatics 18:337–338.
Huson D.H., Rupp R., Scornavacca C. 2010. Phylogenetic networks: concepts, algorithms and applications. Cambridge: Cambridge University Press.
Jónsson H., Schubert M., Seguin-Orlando A., Ginolhac A., Petersen L., Fumagalli M., Albrechtsen A., Petersen B., Korneliussen T.S., Vilstrup J.T., Lear T., Myka J.L., Lundquist J., Miller D.C., Alfarhan A.H., Alquraishi S.A., Al-Rasheid K.A.S., Stagegaard J., Strauss G., Bertelsen M.F., Sicheritz-Ponten T., Antczak D.F., Bailey E., Nielsen R., Willerslev E., Orlando L. 2014. Speciation with gene flow in equids despite extensive chromosomal plasticity. Proc. Natl. Acad. Sci. USA 111:18655–18660.
Klicka L.B., Kus B.E., Title P.O., Burns K.J. 2016. Conservation genomics reveals multiple evolutionary units within Bell's Vireo (*Vireo bellii*). Conserv. Genet. 17:455–471.
Koonin E. V., Makarova K.S., Aravind L. 2001. Horizontal gene transfer in prokaryotes: quantification and classification. Annu. Rev. Microbiol. 55:709–742.
Kuhn M. 2008. Building predictive models in *R* using the caret package. J. Stat. Softw. 28:1–26.
Kumar V., Lammers F., Bidon T., Pfenninger M., Kolter L., Nilsson M.A., Janke A. 2017. The evolutionary history of bears is characterized by gene flow across species. Sci. Rep. 7:46487.
Leaché A.D., Harris R.B., Rannala B., Yang Z. 2014. The influence of gene flow on species tree estimation: a simulation study. Syst. Biol. 63:17–30.
Lek S., Delacoste M., Baran P., Dimopoulos I., Lauga J., Aulagnier S. 1996. Application of neural networks to modelling nonlinear relationships in ecology. Ecol. Model. 90:39–52.
Lek S., Gue J.F. 1999. Artificial neural networks as a tool in ecological modelling, an introduction. Ecol. Model. 120:65–73.
Lemmon A.R., Emme S.A., Lemmon E.M. 2012. Anchored hybrid enrichment for massively high-throughput phylogenomics. Syst. Biol. 61:727–744.
Li G., Davis B.W., Eizirik E., Murphy W.J. 2016. Phylogenomic evidence for ancient hybridization in the genomes of living cats (Felidae). Genome Res. 26:1–11.
Libbrecht M.W., Noble W.S. 2015. Machine learning applications in genetics and genomics. Nat. Rev. Genet. 16:321–332.
Litsios G., Salamin N. 2014. Hybridisation and diversification in the adaptive radiation of clownfishes. BMC Evol. Biol. 14:245.
Losos J.B. 2010. Adaptive radiation, ecological opportunity, and evolutionary determinism. Am. Nat. 175:623–639.
Maddison W.P., Knowles L.L. 2006. Inferring phylogeny despite incomplete lineage sorting. Syst. Biol. 55:21–30.
Mallet J. 2007. Hybrid speciation. Nature 446:279–283.
Mallet J. 2005. Hybridization as an invasion of the genome. Trends Ecol. Evol. 20:229–237.
Mallet J., Besansky N., Hahn M.W. 2016. How reticulated are species? BioEssays. 38:140–149.
Martin S.H., Dasmahapatra K.K., Nadeau N.J., Salazar C., Walters J.R., Simpson F., Blaxter M., Manica A., Mallet J., Jiggins C.D. 2013. Genome-wide evidence for speciation with gene flow in *Heliconius* butterflies. Genome Res. 23:1817–1828.
Matzke N.J. 2013. Probabilistic historical biogeography: new models for founder-event speciation, imperfect detection, and fossils allow improved accuracy and model-testing. Front. Biogeogr. 5.
Matzke N.J. 2014. Model selection in historical biogeography reveals that founder-event speciation is a crucial process in Island Clades. Syst. Biol. 63:951–970.
McCranie J.R. 2011. The snakes of Honduras: systematics, distribution, and conservation. Ithaca: Society for the Study of Amphibians and Reptiles.
McGuire J.A., Linkem C.W., Koo M.S., Hutchison D.W., Lappin A.K., Orange D.I., Lemos-Espinal J., Riddle B.R., Jaeger J.R. 2007. Mitochondrial introgression and incomplete lineage sorting through space and time: phylogenetics of crotaphytid lizards. Evolution 61:2879–2897.
McKelvy A.D., Burbrink F.T. 2017. Ecological divergence in the yellow-bellied kingsnake (*Lampropeltis calligaster*) at two North American biodiversity hotspots. Mol. Phylogenet. Evol. 106:61–72.
Meier J.I., Marques D.A., Mwaiko S., Wagner C.E., Excoffier L., Seehausen O. 2017. Ancient hybridization fuels rapid cichlid fish adaptive radiations. Nat. Commun. 8:14363.
Mirarab S., Warnow T. 2015. ASTRAL-II: coalescent-based species tree estimation with many hundreds of taxa and thousands of genes. Bioinformatics 31:i44-52.
Morafka D.J. 1977. A biogeographical analysis of the Chihuahuan Desert through its herpetofauna. Dordrecht: Springer.
Morales A.E., Carstens B.C. 2018. Evidence that *Myotis lucifugu*s "subspecies" are five non-sister species, despite gene flow: Syst. Biol. 67:773–786.
Morlon H., Potts M.D., Plotkin J.B. 2010. Inferring the dynamics of diversification: A coalescent approach. PloS Biol. 8:e1000493.
Myers E.A., Hickerson M.J., Burbrink F.T. 2017. Asynchronous diversification of snakes in the North American warm deserts. J. Biogeogr. 44:461–474.
Myers E.A., Rodriguez-Robles J.A., Denardo D.F., Staub R.E., Stropoli A., Ruane S., Burbrink F.T. 2013. Multilocus phylogeographic assessment of the California Mountain Kingsnake (*Lampropeltis zonata*) suggests alternative patterns of diversification for the California Floristic Province. Mol. Ecol. 22:5418–5429.
Nee S. 2001. Inferring speciation rates from phylogenies. Evolution. 55:661–668.
Nosil P. 2008. Speciation with gene flow could be common. Mol. Ecol. 17:2103–2106.
Nosil P. 2012. Ecological speciation. Oxford: Oxford University Press.
Oliveira E.F., Gehara M., São-Pedro V.A., Chen X., Myers E.A., Burbrink F.T., Mesquita D.O., Garda A.A., Colli G.R., Rodrigues M.T., Arias F.J., Zaher H., Santos R.M.L., Costa G.C. 2015. Speciation with gene flow in whiptail lizards from a Neotropical xeric biome. Mol. Ecol. 24:5957–75.
Paradis E. 2014. An Introduction to the phylogenetic comparative method. Modern phylogenetic comparative methods and their

application in evolutionary biology. Berlin, Heidelberg: Springer Berlin Heidelberg.
Pigot A.L., Etienne R.S. 2015. A new dynamic null model for phylogenetic community structure. Ecol. Lett. 18:153–63.
Plummer M., Best N., Cowles K., Vines K. 2006. CODA: Convergence diagnosis and output analysis for MCMC. R News. 6:7–11.
Pyron R.A., Burbrink F.T. 2013. Phylogenetic estimates of speciation and extinction rates for testing ecological and evolutionary hypotheses. Trends Ecol. Evol. 28:729–736.
Pyron R.A., Burbrink F.T. 2009. Can the tropical conservatism hypothesis explain temperate species richness patterns? An inverse latitudinal biodiversity gradient in the New World snake tribe Lampropeltini. Glob. Ecol. Biogeogr. 18:406–415.
Pyron R.A., Burbrink F.T. 2010. Hard and soft allopatry: physically and ecologically mediated modes of geographic speciation. J. Biogeogr. 37:2005–2015.
Quental T.B., Marshall C.R. 2010. Diversity dynamics: molecular phylogenies need the fossil record. Trends Ecol. Evol. 25:434–441.
Rabosky D.L. 2010. Extinction rates should not be estimated from molecular phylogenies. Evolution 64:1816–1824.
Rabosky D.L. 2014. Automatic detection of key innovations, rate shifts, and diversity-dependence on phylogenetic trees. PLoS One 9:e89543.
Rabosky D.L. 2017. Phylogenetic tests for evolutionary innovation: the problematic link between key innovations and exceptional diversification. Philos. Trans. R. Soc. Lond. B. Biol. Sci. 372:20160417.
Rabosky D.L., Grundler M., Anderson C., Title P., Shi J.J., Brown J.W., Huang H., Larson J.G. 2014. BAMMtools: an R package for the analysis of evolutionary dynamics on phylogenetic trees. Methods Ecol. Evol. 5:701–707.
Ree R.H., Smith S.A. 2008. Maximum likelihood inference of geographic range evolution by dispersal, local extinction, and cladogenesis. Syst. Biol. 57:4–14.
Revell L.J. 2012. Phytools: an R package for phylogenetic comparative biology (and other things). Methods Ecol. Evol. 3:217–223.
Rheindt F.E., Edwards S. V. 2011. Genetic introgression: an integral but neglected component of speciation in birds. Auk 128:620–632.
Riddle B.R., Hafner D.J. 2006. A step-wise approach to integrating phylogeographic and phylogenetic biogeographic perspectives on the history of a core North American warm deserts biota. J. Arid Environ. 66:435–461.
Ronquist F. 1997. Dispersal-vicariance analysis: a new approach to the quantification of historical biogeography. Syst. Biol. 46:195–203.
Ruane S., Bryson R.W., Pyron R.A., Burbrink F.T. 2014. Coalescent species delimitation in milksnakes (genus *Lampropeltis*) and impacts on phylogenetic comparative analyses. Syst. Biol. 63:231–250.
Rundle H.D., Nosil P. 2005. Ecological speciation. Ecol. Lett. 8:336–352.
Savage J.M. 2002. The amphibians and reptiles of Costa Rica: a herpetofauna between two continents, between two seas. Chicago: University of Chicago Press.
Schluter D. 2000. The ecology of adaptive radiation. Oxford: Oxford University Press.
Schumer M., Rosenthal G.G., Andolfatto P. 2014. How common is homoploid hybrid speciation? Evolution 68:1553–1560.
Seehausen O. 2004. Hybridization and adaptive radiation. Trends Ecol. Evol. 19:198–207.
Sheehan S., Song Y.S., Buzbas E., Petrov D., Boyko A., Auton A. 2016. Deep learning for population genetic inference. PLoS Comput. Biol. 12:e1004845.
De Smet W.H.O. 1981. The nuclear Feulgen-DNA content of the vertebrates (especially reptiles), as measured by fluorescence cytophotometry, with notes on the cell and chromosome size. Acta Zool. Pathol. Antverp. 76:119–167.
Solís-Lemus C., Ané C. 2016. Inferring phylogenetic networks with maximum pseudolikelihood under incomplete lineage sorting. PLoS Genet. 12:e1005896.
Soltis D.E., Buggs R.J.A., Doyle J.J., Soltis P.S. 2010. What we still don't know about polyploidy. Taxon 59:1387–1403.
Soltis P.S., Soltis D.E. 2009. The role of hybridization in plant speciation. Annu. Rev. Plant Biol. 60:561–588.
Stadler T. 2011. Mammalian phylogeny reveals recent diversification rate shifts. Proc. Natl. Acad. Sci. USA 108:6187–6192.
Stenz N.W.M., Larget B., Baum D.A., Ané C. 2015. Exploring tree-like and non-tree-like patterns using genome sequences: an example using the inbreeding plant species *Arabidopsis thaliana* (L.) Heynh. Syst. Biol. 64:809–823.
Trier C.N., Hermansen J.S., Sætre G.-P., Bailey R.I. 2014. Evidence for mito-nuclear and sex-linked reproductive barriers between the hybrid italian sparrow and its parent species. PLoS Genet. 10:e1004075.
Twyford A.D., Ennos R.A. 2012. Next-generation hybridization and introgression. Heredity (Edinb). 108:179–189.
Wan Y., Schwaninger H.R., Baldo A.M., Labate J.A., Zhong G.-Y., Simon C.J. 2013. A phylogenetic analysis of the grape genus (*Vitis* L.) reveals broad reticulation and concurrent diversification during neogene and quaternary climate change. BMC Evol. Biol. 13:141.
Wasserman P.D. 1989. Neural computing: theory and practice. New York: Van Nostrand Reinhold.
Wen D., Yu Y., Hahn M.W., Nakhleh L. 2016a. Reticulate evolutionary history and extensive introgression in mosquito species revealed by phylogenetic network analysis. Mol. Ecol. 25:2361–2372.
Wen D., Yu Y., Nakhleh L., Larget B., Neafsey D., Sharakhov I. 2016b. Bayesian inference of reticulate phylogenies under the multispecies network coalescent. PLoS Genet. 12:e1006006.
Wilson J.S., Pitts J.P. 2010. Illuminating the lack of consensus among descriptions of earth history data in the North American deserts: a resource for biologists. Prog. Phys. Geogr. 34:419–441.
Yu Y., Dong J., Liu K.J., Nakhleh L. 2014. Maximum likelihood inference of reticulate evolutionary histories. Proc. Natl. Acad. Sci. USA 111:16448–16453.
Yu Y., Than C., Degnan J.H., Nakleh L. 2011. Coalescent histories on phylogenetic networks and detection of hybridization despite incomplete lineage sorting. Syst. Biol. 60:138–143.
Zhang W. 2010. Computational ecology: artificial neural networks and their applications. Singapore: World Scientific Publishing Company.
Zhu S., Degnan J.H. 2017. Displayed trees do not determine distinguishability under the network multispecies coalescent. Syst. Biol. 66:283–298.